IEEE Access
Multidisciplinary | Rapid Review | Open Access Journal

Received February 4, 2019, accepted March 8, 2019, date of publication March 18, 2019, date of current version April 5, 2019.

*Digital Object Identifier 10.1109/ACCESS.2019.2905716*

# A Method for Gravitational Apparent Acceleration Identification and Accelerometer Bias Estimation

**XIXIANG LIU, SONGBING WANG, XIAOLE GUO, WENQIANG YANG, AND GUANGFU XU**

School of Instrument Science and Engineering, Southeast University, Nanjing 210096, China
Key Laboratory of Micro-inertial Instrument and Advanced Navigation Technology, Ministry of Education, Southeast University, Nanjing 210096, China

Corresponding author: Xixiang Liu (scliuseu@163.com)

This work was supported in part by the Six talent peaks project of Jiangsu Providence under Grant 2016-HYGC-001, in part by the Qingdao National Laboratory for Marine Science and Technology under Grant QNLM2016ORP0406, and in part by the Key Research and Development Program of Jiangsu Providence under Grant BE2016176.

**ABSTRACT** Accelerometer bias in an inertial navigation system (INS) is the key factor determining the navigation accuracy. Two methods, named separated calibration and system calibration are always used for acceleration bias calibration. The former one needs a high precision turntable to provide reference and the latter cannot estimate accelerometer bias along horizontal direction because of coupling effects between horizontal misalignment angles and horizontal accelerometer bias. In this paper, a new estimation method is designed to estimate accelerometer biases and acquire high horizontal alignment accuracy without a turntable. In the proposed method, different expressions about gravity and accelerometer biases in an inertial frame are analyzed and coupling models about gravity and biases are constructed. Then, measurements from gyroscopes and accelerometers are used to construct gravitational apparent acceleration and Kalman filter used to estimate parameters describing apparent acceleration and estimate accelerometer bias. The simulation and turntable tests show that when the carrier is without translational but with swinging motion, the proposed method can finish gravitational apparent acceleration identification and accelerometer bias estimation effectively at the same time, and when the reconstructed gravitational apparent acceleration used for alignment, horizontal alignment errors can nearly approach zeros.

**INDEX TERMS** Accelerometer bias, gravitational apparent acceleration, initial alignment, Kalman filter, srapdown inertial navigation system.

## I. INTRODUCTION

Inertial navigation system (INS) is a kind of navigation method based on integral working mode. In navigation process, sensor errors including gyroscope and accelerometer biases will be accumulated to be positioning errors with the navigation time. Generally, constant biases of gyroscopes and accelerometers are the main error sources causing navigation errors [1]–[3].

Sensor errors are always existed, thus sensor should be calibrated and compensated before they are delivered from factories. Meanwhile, sensor errors will be changed after using or stored for a long time or the changes of working environment, thus initial alignment including sensor calibration or estimation should be executed before navigation, and online calibration should be executed during navigation to guarantee the navigation precision. Factory calibration, named calibration always compares senor measuring data with reference data from high-precision turntable equipment to acquire sensor errors. Calibrations before or during navigation are called system calibration. In system calibration, navigation data from navigation system or reference system are compared and sensor errors are deduced with filters, such as Kalman filter. Error propagation models and filter are two main factors which determines the accuracy of estimated sensor errors. In this paper, sensor calibration before navigation is studied and this calibration are always executed in the field.

Separated calibration always needs high-precision turntable which cannot be satisfied in working field such as dock or sea, then system calibration become the first choice for those calibrations before navigation. In system calibration, aided navigation data from other navigation system are always used as reference, and velocity is the most common and accessible data. With velocity matching mode, velocities from INS and aided system are compared. Then the misalignment and sensor errors are deduced with the help

The associate editor coordinating the review of this manuscript and approving it for publication was Bora Onat.

of error propagation equation and filter [4], [5]. In SINS, accelerometer bias will cause velocity error after integration and horizontal misalignment angles will also cause velocity error because of the projected gravitational acceleration. That means there is a coupling effect between accelerometer bias and INS horizontal misalignment angles. Similarly, there is a coupling between east gyro bias, north accelerometer bias and azimuth misalignment angle. Decoupling sensors errs and misalignment angles with velocity matching always require various kinds of maneuvers, such as acceleration, deceleration, steering, winged wing or somersault [6], [7]. Unfortunately, for those ships, vehicles or large aircrafts, above maneuvers cannot be executed. Other perspectives are needed to solve the problem of decoupling sensor errors and misalignment angles. In this paper, a novel calibration method for accelerometer bias is designed and verified.

Recently, an initial alignment method based on gravitational apparent acceleration or velocity has been focused [8]–[13]. In this method, initial alignment of SINS solving attitude matrix between navigation frame and body frame has been translated to solve attitude matrix between those navigation frame and body frame at start time, and frames at start time are defined as inertial frames in this paper. In inertial frame, gravity in navigation frame will be projected as a cone that means apparent accelerations in inertial frame are all non-collinear vectors. When any two gravitational apparent acceleration vectors in inertial navigation frame and initial body frame are calculated, dual vector attitude determination method can be used to solve matrix between these two frames. It is believed as an excellent coarse alignment method to fulfill alignment with a swing base.

In this method, noises in gyroscopes will be smoothed with integration but noise in accelerometers will be directly projected into apparent acceleration as noise. And noises in apparent acceleration will bring two vectors possible collinear and lead fail alignment or decreasing alignment accuracy. Aiming to solving this problem, extensive research have been carried out and many achievements have be gotten [9], [13]–[16]. In [9], theoretical rules about gravitational acceleration has been deduced when the carrier is without translation motion, and it is believed parameters describing apparent acceleration are unknown but fixed data, then calculated apparent acceleration gotten with gyroscopes and accelerometers can be used as measured data, theoretical rules used as measured matrix and recursive least square algorithm as filter to identify parameters describing apparent acceleration. After parameters in theoretical rules have been identified, apparent acceleration can be reconstructed without effects of noises. With those reconstructed acceleration, alignment accuracy can reach those highest accuracy determined by sensor errors.

Based on rules describing apparent motion, in this paper coupling model about apparent acceleration and accelerometer bias are deduced firstly. And an estimating method for parameters in apparent motion and sensor biases are designed and verified. Simulation and turntable tests indicates that gravitational apparent acceleration can be identified and accelerometer bias can be estimated at the same time, and horizontal alignment errors can approach nearly zeros when those reconstructed apparent accelerations minus accelerometer biases are used for alignment.

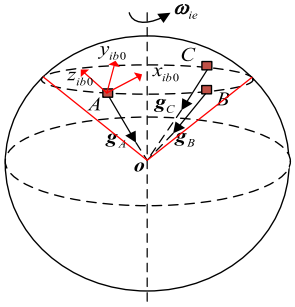


**FIGURE 1.** Demonstration of gravitational apparent motion.

The rest of this paper is organized as follows. In Section II gravitational apparent acceleration and coupling model about apparent acceleration/accelerometer bias is described. And in Section III, the method to estimate parameters about apparent acceleration and accelerometer biases using recursive least square algorithm is designed and analyzed with analytic and observability methods. Simulation and turntable tests are carried out in Section IV and conclusions are given in Section V.

## II. GRAVITATIONAL APPARENT ACCELERATION/ ACCELEROMETER BIAS COUPLING MODEL

### A. GRAVITATIONAL APPARENT ACCELERATION MODEL

Different from apparent motion of gyroscope, gravitational apparent motion defined in [9] is as the direction change of gravity with the earth's rotation in inertial frame. As illustrated in FIGURE 1, $A$, $B$ and $C$ are the locations of the same point on the earth at different moments in inertial space, and $\boldsymbol{g}_A$, $\boldsymbol{g}_B$ and $\boldsymbol{g}_C$ are all non-collinear gravity vectors of $A$, $B$ and $C$ respectively. After the earth rotating from west to east, the direction of gravity vector of the same point forms a complete cone.

When the carrier is without translational motion, the theoretical value measured by accelerometer is the projection of gravity vector in body frame $b$ and two vectors have equal magnitude but opposite direction as follows:

$$\boldsymbol{g}^b(t) = -\boldsymbol{f}^b(t) \tag{1}$$

where $b$ denotes body frame. Similarly, in navigation frame $n$, there is $\boldsymbol{f}^n(t) = -\boldsymbol{g}^n(t) = \begin{bmatrix} 0 & 0 & g \end{bmatrix}^T$.

In [9], gravitational apparent acceleration in inertial frame is expressed as follows:

$$\boldsymbol{f}^i(t) = \boldsymbol{C}_n^i \boldsymbol{f}^n(t) = \boldsymbol{C}_{i_{n0}}^i \boldsymbol{C}_{e_0}^{i_{n0}} \boldsymbol{C}_e^{e_0}(t) \boldsymbol{C}_n^e(t) \boldsymbol{f}^n(t) \tag{2}$$

where $i$ denotes inertial frame; $i_{n0}$ is auxiliary navigation frame aligned with frame $n$ at start-up of the alignment; $e_0$ is

auxiliary earth frame aligned with $e$ frame at start-up of the alignment; $e$ denotes earth frame at current time; $\boldsymbol{C}_B^A$ means attitude matrix from frame $B$ to frame $A$. Among the matrixes discussed above, $\boldsymbol{C}_{i_{n0}}^{i}$ and $\boldsymbol{C}_{e_0}^{i_{n0}}$ are constant values and $\boldsymbol{C}_n^e(t)$ is also constant when the carrier is without translational motion; $\boldsymbol{C}_e^{e_0}(t)$ is a matrix which is related to time $t$ and the earth rotation rate. Thus, Eq. (2) can be expanded as follows:

$$\begin{aligned}\boldsymbol{f}^i(t) &= \boldsymbol{C}_{i_{n0}}^{i}\boldsymbol{C}_{e_0}^{i_{n0}}\boldsymbol{C}_e^{e_0}(t)\,\boldsymbol{C}_n^e(t)\boldsymbol{f}^n(t)\\ &= \begin{bmatrix} a_{11} & a_{12} & a_{13}\\ a_{21} & a_{22} & a_{23}\\ a_{31} & a_{32} & a_{33}\end{bmatrix}\begin{bmatrix} b_{11} & b_{12} & b_{13}\\ b_{21} & b_{22} & b_{23}\\ b_{31} & b_{32} & b_{33}\end{bmatrix}\\ &\quad\times\begin{bmatrix}\cos(\omega_{ie}t) & -\sin(\omega_{ie}t) & 0\\ \sin(\omega_{ie}t) & \cos(\omega_{ie}t) & 0\\ 0 & 0 & 1\end{bmatrix}\begin{bmatrix} c_{11} & c_{12} & c_{13}\\ c_{21} & c_{22} & c_{23}\\ c_{31} & c_{32} & c_{33}\end{bmatrix}\begin{bmatrix}0\\0\\g\end{bmatrix}\\ &= \begin{bmatrix} A_{11} & A_{12} & A_{13}\\ A_{21} & A_{22} & A_{23}\\ A_{31} & A_{32} & A_{33}\end{bmatrix}\begin{bmatrix}\cos(\omega_{ie}t)\\ \sin(\omega_{ie}t)\\ 1\end{bmatrix}\end{aligned} \tag{3}$$

where $a_{11\sim33}$, $b_{11\sim33}$, $c_{11\sim33}$ and $A_{11\sim33}$ are all constant values; $\omega_{ie}$ and $g$ are the earth rotation rate and the modulus of gravity acceleration respectively; $t$ is initial alignment time from start-up. When the position of the carrier is determined, parameters $A_{11\sim33}$ are only related to the selection of the inertial system. If a special inertial frame is selected, parameters $a_{11\sim33}$, $b_{11\sim33}$, $c_{11\sim33}$ and $A_{11\sim33}$ are determined and more details can be referred in [9].

### B. COUPLING MODEL OF GRAVITATIONAL APPARENT ACCELERATION /ACCELEROMETER BIAS

Choosing the body frame at start-up of the alignment as inertial frame, $i$ can be specified as $i_{b0}$. And calculated gravitational apparent acceleration can be obtained based on the measurements from gyroscopes and accelerometers as follows:

$$\hat{\boldsymbol{f}}^{i_{b0}}(t) = \hat{\boldsymbol{C}}_b^{i_{b0}}(t)\tilde{\boldsymbol{f}}^b(t) \tag{4}$$

In Eq. (4), $\hat{\boldsymbol{f}}^{i_{b0}}(t)$ is the calculated value of gravitational apparent acceleration; $\hat{\boldsymbol{C}}_b^{i_{b0}}$ is the calculated attitude matrix from body frame at current time to inertial frame; $\tilde{\boldsymbol{f}}^b(t)$ is the measurement with accelerometers. In Eq. (4), $\hat{\boldsymbol{C}}_b^{i_{b0}}$ can be obtained as follows:

$$\dot{\hat{\boldsymbol{C}}}_b^{i_{b0}} = \hat{\boldsymbol{C}}_b^{i_{b0}}\left(\tilde{\boldsymbol{\omega}}_{ib}^b\times\right) \tag{5}$$

where $\tilde{\boldsymbol{\omega}}_{ib}^b$ is the measurement with gyroscopes.

Considering accelerometer bias and random noise, the accelerometer measurement model can be expressed as follows:

$$\tilde{\boldsymbol{f}}^b = \boldsymbol{f}^b + \boldsymbol{\nabla}^b + \boldsymbol{\eta}^b \tag{6}$$

where $\boldsymbol{\nabla}^b$ and $\boldsymbol{\eta}^b$ are accelerometer bias and random noise respectively. When taking the Eq. (6) into the Eq. (4), gyroscope errors have similar effects on every element in Eq. (6), and then Eq. (4) can be rewrite as follows with ignoring gyroscope errors:

$$\begin{aligned}\hat{\boldsymbol{f}}^{i_{b0}}(t) &= \boldsymbol{C}_b^{i_{b0}}(t)\left(\boldsymbol{f}^b + \boldsymbol{\nabla}^b + \boldsymbol{\eta}^b\right)\\ &\approx \boldsymbol{C}_b^{i_{b0}}(t)\boldsymbol{f}^b + \boldsymbol{C}_b^{i_{b0}}(t)(t)\,\boldsymbol{\nabla}^b + \boldsymbol{C}_b^{i_{b0}}(t)\,\boldsymbol{\eta}^b\end{aligned} \tag{7}$$

Eq. (7) indicates that the calculated values of gravity apparent acceleration consist of the true value, bias and random noise.

In [9], above Eqs. (3) and (4) are selected as measurement matrix and measured data to estimate parameters $A_{11}\sim A_{33}$ with recursive least square method. Though random noise can be effectively suppressed, biases $\boldsymbol{C}_b^{i_{b0}}(t)\,\boldsymbol{\nabla}^b$ as shown in Eq. (7) still exist. Thus sensor bias will exist in identified parameters and reconstructed apparent accelerations. Thus highest alignment accuracy will be determined by sensor errors just as those methods of compass alignment method and fusion method based on Kalman filter. With this method, horizontal alignment accuracies are as follows [9]:

$$\begin{cases}\phi_E = \dfrac{\nabla_N}{g}\\ \phi_N = -\dfrac{\nabla_E}{g}\end{cases} \tag{8}$$

where $\phi_E$ and $\phi_N$ are eastern and northern misalignment angles respectively; $\nabla_E$ and $\nabla_N$ are the equivalent accelerometer errors along eastern and northern directions respectively.

## III. IDENTIFICATION ALGORITHM FOR GRAVITY APPARENT ACCELERATION AND ACCELEROMETERS BIAS

Analysis in Section II indicates that gravitational apparent accelerations own fixed rules and expression when the carrier is without translational motion. Further analysis in this section will indicates that when the carrier is without translational but swinging motion, gravity and accelerometer biases will own different rules in inertial frame. Base on this, a new estimation method for parameters describing apparent acceleration and accelerometer biases has been designed as follows.

### A. MODELS OF ACCELEROMETER BIAS ESTIMATION AND PARAMETERS IDENTIFICATION

Taking Eq. (3) into Eq. (7), the calculated apparent acceleration can be expressed as follows:

$$\begin{aligned}\hat{\boldsymbol{f}}^{i_{b0}}(t) &= \boldsymbol{C}_b^{i_{b0}}(t)\boldsymbol{f}^b + \boldsymbol{C}_b^{i_{b0}}(t)\,\boldsymbol{\nabla}^b + \boldsymbol{C}_b^{i_{b0}}(t)\,\boldsymbol{\eta}^b\\ &= \boldsymbol{C}_n^{i_{b0}}(t)\boldsymbol{f}^n + \boldsymbol{C}_b^{i_{b0}}(t)\,\boldsymbol{\nabla}^b + \boldsymbol{C}_b^{i_{b0}}(t)\,\boldsymbol{\eta}^b\\ &= \begin{bmatrix} A_{11} & A_{12} & A_{13}\\ A_{21} & A_{22} & A_{23}\\ A_{31} & A_{32} & A_{33}\end{bmatrix}\begin{bmatrix}\cos(\omega_{ie}t)\\ \sin(\omega_{ie}t)\\ 1\end{bmatrix}\\ &\quad+\begin{bmatrix} C_{11} & C_{12} & C_{13}\\ C_{21} & C_{22} & C_{23}\\ C_{31} & C_{32} & C_{33}\end{bmatrix}\begin{bmatrix}\nabla_x^b\\ \nabla_y^b\\ \nabla_z^b\end{bmatrix}+\begin{bmatrix}\eta_x^{i_{b0}}\\ \eta_y^{i_{b0}}\\ \eta_z^{i_{b0}}\end{bmatrix}\end{aligned} \tag{9}$$

where $C_{11\sim33}$ are the elements of matrix $\boldsymbol{C}_b^{i_{b0}}$; $\nabla_{x\sim z}^b$ are projections of $\boldsymbol{\nabla}^b$ in frame $b$; $\eta_{x\sim z}^{i_{b0}}$ are random noise and $\boldsymbol{C}_b^{i_{b0}}(t)\,\boldsymbol{\eta}^b$ are their projections in frame $i_{b0}$. Gravity accelerations are separated from accelerometers bias in Eq. (9). When $A_{11}\sim A_{33}$ and $\nabla_{x\sim z}^b$ are selected as state vector and $\hat{\boldsymbol{f}}^{i_{b0}}(t)$ are as measurement vector, parameters in apparent acceleration and accelerometer bias can be estimated with that similar method in [9]. However, whether the gravitational apparent motion can be decoupled from the accelerometer bias or not is needed to be further studied.

Considering that gravity vector is independent of the body frame while the accelerometers are installed on carrier and accelerometer bias are along axes of carrier frame, rewrite Eq. (7) as follows:

$$\begin{aligned}\hat{\boldsymbol{f}}^{i_{b0}}(t) &= \boldsymbol{C}_b^{i_{b0}}(t)\boldsymbol{f}^b + \boldsymbol{C}_b^{i_{b0}}(t)\,\boldsymbol{\nabla}^b + \boldsymbol{C}_b^{i_{b0}}(t)\,\boldsymbol{\eta}^b \\ &= \boldsymbol{C}_n^{i_{b0}}(t)\boldsymbol{f}^n + \boldsymbol{C}_n^{i_{b0}}\boldsymbol{C}_b^n(t)\,\boldsymbol{\nabla}^b + \boldsymbol{\eta}^{i_{b0}} \\ &= \boldsymbol{C}_n^{i_{b0}}(t)\left(\boldsymbol{f}^n + \boldsymbol{C}_b^n(t)\,\boldsymbol{\nabla}^b\right) + \boldsymbol{\eta}^{i_{b0}}\end{aligned} \tag{10}$$

If carrier is assumed without swinging motions, $\boldsymbol{C}_b^n(t)$ is a constant matrix and $\boldsymbol{C}_b^n(t)\,\boldsymbol{\nabla}^b$ is a constant vector just as that of $\boldsymbol{f}^n$. That mean $\boldsymbol{f}^n$ and $\boldsymbol{C}_b^n(t)\,\boldsymbol{\nabla}^b$ have the same expression in frame $i_{b0}$. Thus $\boldsymbol{f}^n$ and $\boldsymbol{C}_b^n(t)\,\boldsymbol{\nabla}^b$ cannot be decoupled with Eq. (10).

If carrier is assumed with swinging motions, $\boldsymbol{C}_b^n(t)$ and $\boldsymbol{C}_b^n(t)\,\boldsymbol{\nabla}^b$ are both time-varying matrix and vector, thus $\boldsymbol{f}^n$ and $\boldsymbol{C}_b^n(t)\,\boldsymbol{\nabla}^b$ display different forms in frame $i_{b0}$. Specifically, in frame $n$, $\boldsymbol{f}^n$ is a fixed one and $\boldsymbol{C}_b^n(t)\,\boldsymbol{\nabla}^b$ is a periodic data, then in $i_{b0}$, $\boldsymbol{f}^n$ can be expressed with Eq. (3) and $\boldsymbol{C}_b^n(t)\,\boldsymbol{\nabla}^b$ is periodic components superimposed on gravitational apparent motion. Above characters make it possible to complete gravitational apparent motion identification and accelerometer bias estimation at the same time. Further analysis will be executed in Section IV.

### B. ESTIMATION FOR PARAMETERS IN GRAVITATIONAL APPARENT ACCELERATION AND ACCELEROMETER BIAS

Taking $A_{11}\sim A_{33}$ and $\nabla_{x\sim z}^b$ as state vector:

$$\boldsymbol{X} = \left[\,A_{11}\ A_{12}\ A_{13}\ A_{21}\ A_{22}\ A_{23}\ A_{31}\ A_{32}\ A_{33}\ \nabla_x^b\ \nabla_y^b\ \nabla_z^b\,\right]^{\mathrm{T}} \tag{11}$$

Above analysis shows that when the inertial frame is fixed, $A_{11}\sim A_{33}$ and $\nabla_{x\sim z}^b$ are constant values and $\boldsymbol{X}$ can be seen as a constant vector in a short time, then the system state equation can be expressed as:

$$\boldsymbol{X}_k = \boldsymbol{X}_{k-1} \tag{12}$$

Taking the calculated gravitational apparent acceleration as measurement vector,

$$\boldsymbol{Z} = \hat{\boldsymbol{f}}^{i_{b0}} = \left[\begin{array}{ccc}\hat{f}_x^{i_{b0}} & \hat{f}_y^{i_{b0}} & \hat{f}_z^{i_{b0}}\end{array}\right]^{\mathrm{T}} \tag{13}$$

According to the Eq. (9), the measurement matrix can be deduced as follows (14), as shown at the bottom of this page, where $C_{11\sim33}$ are the elements of matrix $\boldsymbol{C}_b^{i_{b0}}$. Based on the above equations, recursive least square algorithm can be used to estimate the above state variables. The on-line estimation filter based on recursive least square algorithm is as follows [9]:

$$\begin{cases}\boldsymbol{K}_k = \boldsymbol{P}_{k-1}\boldsymbol{H}_k^{\mathrm{T}}\left(\boldsymbol{H}_k\boldsymbol{P}_{k,k-1}\boldsymbol{H}_k^{\mathrm{T}} + \boldsymbol{R}_k\right)^{-1} \\ \boldsymbol{X}_k = \boldsymbol{X}_{k-1} + \boldsymbol{K}_k\left(\boldsymbol{Z}_k - \boldsymbol{H}\boldsymbol{X}_k\right) \\ \boldsymbol{P}_k = \left[\boldsymbol{I} - \boldsymbol{K}_k\boldsymbol{H}_k\right]\boldsymbol{P}_{k-1}\end{cases} \tag{15}$$

### C. ANALYSIS OF THE OBSERVABILITY

Eq. (10) indicates that the above estimation algorithm can be considered as a linear constant system, which can be analyzed by the observability of the system to provide decoupling criterion of gravitational apparent motion and accelerometer bias. At present, the research on the observability of the system is mature. Establishing the observability discriminant array of the linear system and judging the rank of it, then the observability of the linear system can be simply determined.

For the following linear systems with no input:

$$\begin{cases}\dot{\boldsymbol{X}} = \boldsymbol{A}\boldsymbol{X} \\ \boldsymbol{Z} = \boldsymbol{H}\boldsymbol{X}\end{cases} \tag{16}$$

where $\boldsymbol{X}$ is a state vector with the dimension $n\times 1$, $\boldsymbol{Z}$ is an output vector with the dimension $m\times 1$, $\boldsymbol{A}$ is a matrix with the dimension $n\times n$, $\boldsymbol{H}$ is a matrix with the dimension $m\times n$. When all elements of initial state $\boldsymbol{X}(0)$ can be determined within a finite time interval by $\boldsymbol{Z}(t)$, the system described by Eq. (16) is completely observable.

For linear time invariant systems, the observable Gram matrix is follows [17]:

$$\boldsymbol{W}(0\sim t) = \int_0^t e^{\boldsymbol{A}^{\mathrm{T}}\tau}\boldsymbol{H}^{\mathrm{T}}\boldsymbol{H}e^{\boldsymbol{A}\tau}d\tau \tag{17}$$

The necessary condition for its complete observation is that $t(0)$ satisfies:

$$\mathrm{rank}\left(\boldsymbol{W}(0\sim t)\right) = n \tag{18}$$

where $\boldsymbol{W}(0\sim t)$ is a concept related to the energy of the output signal. If Gram matrix is full rank when $t > t_0$, the system is completely observable. On the contrary, the system cannot be observed completely. Based on the rank of Gram matrix, the observability of quantities can be judged.

$$\boldsymbol{H} = \left[\begin{array}{ccccccccccccc}\cos(\omega_{ie}t) & \sin(\omega_{ie}t) & 1 & 0 & 0 & 0 & 0 & 0 & 0 & C_{11} & C_{12} & C_{13} \\ 0 & 0 & 0 & \cos(\omega_{ie}t) & \sin(\omega_{ie}t) & 1 & 0 & 0 & 0 & C_{21} & C_{22} & C_{23} \\ 0 & 0 & 0 & 0 & 0 & 0 & \cos(\omega_{ie}t) & \sin(\omega_{ie}t) & 1 & C_{31} & C_{32} & C_{33}\end{array}\right] \tag{14}$$

The system described in Eq. (12) is a linear constant system, and $\boldsymbol{A} = \mathbf{0}_{12\times12}$ in Eq. (16). Eq. (17) can be simplified to follow:

$$\boldsymbol{W}(0 \sim t) = \int_0^t \boldsymbol{H}^T \boldsymbol{H} d\tau \tag{19}$$

Calculating the rank of the Gram matrix which is obtained through Eq. (19) and the observability of the system can be judged. Analysis of the designed method can be seen in Section IV A.

## IV. SIMULATION AND TURNTABLE TEST

### A. SIMULATION TEST

#### 1) SIMULATION SETTING

Take ship as an example and it is assumed the ship without translational motion. Two different swinging motions are analyzed. The first one assumes the ship to be static without any angle motion and the second assumes the ship is with swinging motion following the function $A\sin(2\pi f \cdot t + \beta_0) + \theta_0$, where $A$ and $f$ are the amplitude and frequency of swinging while $\beta_0$ and $\theta_0$ are the initial phase and attitude angle. The specific swinging parameters are shown in TABLE 1. And the initial longitude and latitude of ship are set as 118° and 32° respectively.

**TABLE 1. Swinging parameters setting.**

| | Pitch | Roll | Yaw |
|---|---|---|---|
| Amplitude(°) | 6 | 13 | 8 |
| Cycle ( s ) | 10 | 8 | 8 |
| Initial Phase(°) | 0 | 0 | 0 |
| Initial Angle(°) | 2 | 6 | 5 |

Based on the above ideal motions, the ideal outputs of accelerometers and gyroscopes can be gotten by back-stepping of navigation algorithm. When sensor constant errors and random errors are added into the ideal outputs, the real sensor data can be obtained. The update cycle of sensor data is set as 10 ms. The sensor errors are shown in TABLE 2 and random noise satisfies white noise hypothesis. The simulation lasts for 4000s. Observability is analyzed by using Eq. (19) in section 3.3 and estimation for sensor errors is fulfilled by using least squares recursive method

**TABLE 2. Sensor errors setting.**

| | Gyro bias(°/h) | | Acce bias (ug) | |
|---|---|---|---|---|
| | Constant | Random | Constant | Random |
| x-axis | 0.01 | 0.01 | 60 | 50 |
| y-axis | 0.01 | 0.01 | 150 | 50 |
| z-axis | 0.01 | 0.01 | 260 | 50 |

which introduced in Section III B. Alignment algorithm in Section III B from [9] is used for initial alignment.

#### 2) ANALYSIS OF SYSTEM OBSERVABILITY

The ranks of system observability matrix under two cases are calculated by using Eq. (19) as shown in FIGURE 2. FIGURE 2(a) and (b) correspond to the swinging base and static base respectively.

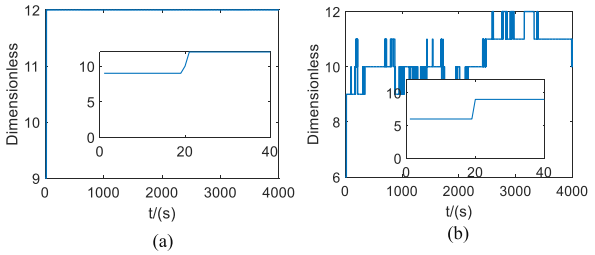


**FIGURE 2. The rank of system observability matrix. (a) Swinging conditions. (b) Static base conditions.**

FIGURE 2(a) indicates that ranks of the matrix in the first 20 seconds and later is 9 and 12 respectively when the ship is with swinging motion, thus the system can be completely observed after 20 seconds. FIGURE 2(b) shows that the rank of the system observation matrix is less than the dimension of the system state, thus the system cannot be completely observed at most time when the ship is under static base conditions. That is to say, gravitational apparent motion and accelerometer bias cannot be decoupled.

Based on above analysis, the simulation and tests of gravitational apparent motion identification and accelerometer bias estimation are carried out only in swinging conditions in the following section.

#### 3) RESULTS OF SIMULATION

FIGURE 3 shows the estimated value for accelerometer bias under the condition of swinging base without translational motion. In FIGURE 3, real lines represent the estimation of accelerometer biases and dotted lines represent the true value of biases. Curves in FIGURE 3 show that the bias of three accelerometers can be estimated when the ship is without translational motion but with swinging motion, and

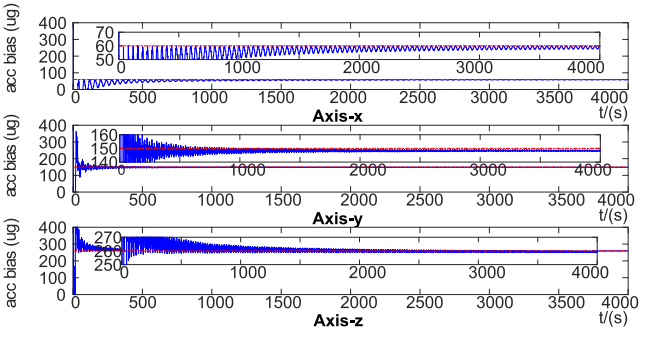


**FIGURE 3. Estimation for accelerometer bias with simulation.**

**TABLE 3.** Statistical data about errors of two methods.

| Mean | | Pitch | Roll |
|---|---|---|---|
| Theoretical alignment accuracy ( ° ) | | 0.008594 | -0.003437 |
| Simulation alignment accuracy ( ° ) | method 1 | 0.008687 | -0.003398 |
| | method 2 | 0.000069 | -0.000218 |

the difference between estimated and the true values are very small.

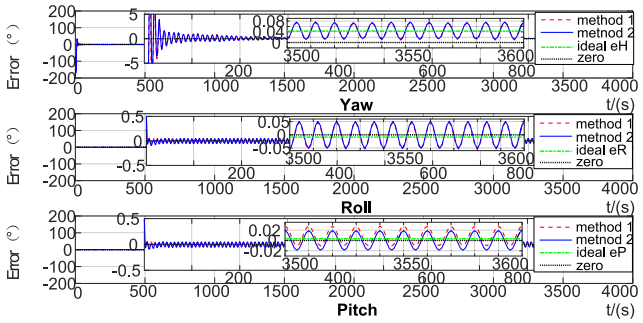


**FIGURE 4.** Errors of alignment of two methods with simulation.

FIGURE 4 shows alignment errors by using analytical alignment method and reconstructed gravitational apparent acceleration by parameters $A_{11} \sim A_{33}$. In FIGURE 4, dotted lines represent alignment results fulfilled with method in [9] (defined as method 1), and solid lines represent alignment results with proposed method (defined as method 2). In method 2, accelerometer bias will be minuses from reconstructed apparent acceleration with estimation method automatically. And ideal eP, ideal eR and ideal eH are the smallest alignment errors of pitch, roll and yaw determined by sensor errors. Zero lines are also displayed in FIGURE 4 for the convenience of comparing different alignment results. Statistics of two methods from time 3500s to 4000s are listed in TABLE 3. The curves in FIGURE 4 and statistical data in TABLE 3 show that the accuracy of the horizontal alignment is greatly improved after the accelerometer bias being separated from the value of gravitational apparent motion, and the error of the horizontal misalignment angle can nearly approach zero.

### B. TURNTABLE TEST

#### 1) TEST SETTING

The turntable used for test is shown in FIGURE 5. In this turntable, the rate controlling accuracy is $\pm 0.0005°/s$ and angle measuring accuracy is $\pm 0.0001°/s$. Besides the turntable can respond to external time-synchronization signal and provide angle information via serial communication port. In the test, the inner, intermediate and outer frames of the turntable are used to simulate the ship's roll, pitch and yaw respectively. The swinging parameters are set in TABLE 4.

**TABLE 4.** Swinging parameter of turntable.

| | Inner frame | Intermediate frame | Outer frame |
|---|---|---|---|
| Amplitude(°) | 6 | 13 | 8 |
| Frequency (Hz) | 0.1333 | 0.2778 | 0.1087 |

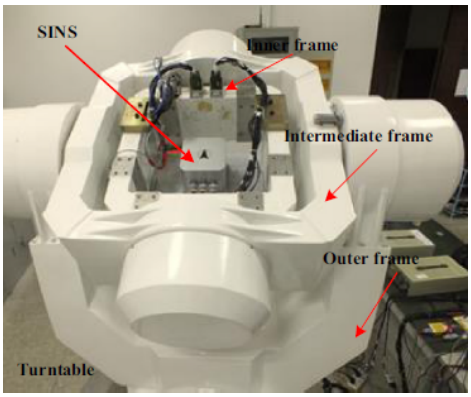


**FIGURE 5.** The turntable and SINS.

As shown in FIGURE 5, inertial measurement unit (IMU) is installed in the turntable with the x, y and z axes coinciding with the axes of intermediate, inner and outer frame respectively. According to [18], sensors' zero bias, scale factors, coupling coincident and installing error can be calculated and compensated by the exactly calibration. In the test, the update frequency of turntable data are both 200 Hz and angle information of the turntable will be provided every 5 ms which is used to compare the calculated values and evaluate the alignment accuracy. The error between angle information of the turntable and the calculated values caused by time synchronization is compensated by interpolation or recursion. The alignment experiment data is obtained after one boot. In this test, above error except accelerometer bias are calibrated and compensated and accelerometer biases are unknown.

#### 2) RESULTS OF TURNTABLE TEST

Turntable test lasts for 2500 s. Results of accelerometer bias and initial alignment errors with method 2 are displayed in FIGURE 6 and FIGURE 7 with solid lines respectively. Also alignment errors with method 1 are displayed with dashed lines in FIGURE 7. TABLE 5 and TABLE 6 show the statistical data about accelerometer biases and alignment errors from 2000s to 2500s.

Curves in FIGURE 6 show the estimation of accelerometer biases convergent after about 500 s and keep stable. And curves in FIGURE 7 show that horizontal alignment errors with method 2 approach nearly zeros.

In turntable test, estimation of accelerometer biases cannot be evaluated directly because of the unknown accelerometer biases. But if we compare the alignment difference between

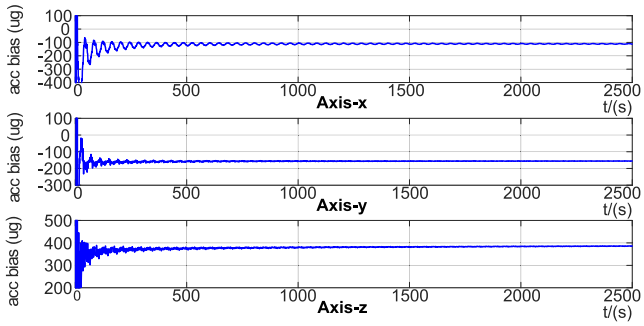


**FIGURE 6.** Estimation results of accelerometer bias with turntable test.

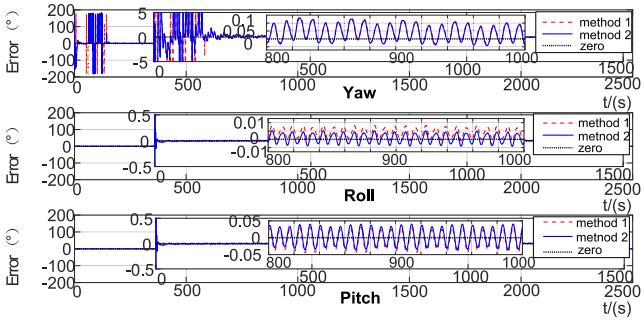


**FIGURE 7.** Accuracy of attitude angle alignment with turntable test.

**TABLE 5.** Mean of accelerometer bias.

| X axis ( ug ) | Y axis ( ug ) | Z axis ( ug ) |
|---|---|---|
| -110.731057 | -155.645403 | 384.942223 |

**TABLE 6.** Results errors of turntable.

| Mean | | Pitch | Roll |
|---|---|---|---|
| Theoretical alignment accuracy ( ° ) | | -0.008917 | 0.006344 |
| Simulation alignment accuracy ( ° ) | method 1 | -0.006205 | 0.007917 |
| | method 2 | 0.000520 | 0.000458 |

two methods as shown in TABLE 5 and estimated accelerometer biases, it can be found they satisfy the relation described in Eq. (8).

Based on above analysis, it can be seen the method designed in this paper can effectively estimate the accelerometer bias and complete the attitude alignment work. The errors of the horizontal alignment are close to zero.

### C. FURTHER ANALYSIS ON SIMULATION AND TURNTABLE TEST

Results of simulation and turntable test show the alignment accuracy of yaw are changed with proposed method and the accuracy of estimated accelerometer biases are not affected by gyroscope errors.

The reasons are as follows: 1) the proposed method does nothing on the constant error of eastern gyroscope, thus the accuracy of yaw will not be change; 2) constant errors in gyroscopes will accumulated as $\delta \boldsymbol{C}_b^{ib0}$ that will change the rules gravitational apparent acceleration, the influence on gravity and accelerometer bias are the same, thus the estimated accelerometer biases are not affected by gyroscope errors.

## V. CONCLUSIONS

In this paper, a new method for parameters describing gravitational apparent motion identification and accelerometer bias estimation are designed. With this method, high accuracy turntable used in separated calibration is not needed and the problem about un-observable level accelerometer bias when velocity matching is used in system calibration can be solved.

The principles behind the proposed method are as follows: when the ship is with swinging but without translational motion, gravity and accelerometer bias have different expression in inertial frame. In inertial frame, accelerometer bias is a periodic component superimposed on gravitational apparent acceleration. Based on this, when rules of apparent acceleration is used as measurement equation and calculated apparent motion is as measurement data and recursive least square algorithm as filter, parameters describing apparent acceleration and accelerometer bias can be estimated effectively. Simulation and turntable test both show the validity of proposed method and when biases are decoupled from calculated apparent motion, horizontal alignment error approaches nearly to zero.

## REFERENCES

[1] Z. Lu and X. Wang, "Error analysis and calibration of systematic dual-axis rotation-modulating SINS," *J. Chin. Inertial Technol.*, vol. 18, no. 2, pp. 135–141, 2010.

[2] Z. Xiong, J. Y. Liu, and X. Y. Lin, "Inertial instrument error compensation technology in the laser gyro strapdown inertial navigation system," *J. Shanghai Jiaotong Univ.*, vol. 37, no. 11, pp. 1795–1799, 2003.

[3] P. B. Reddy, "On stationary and nonstationary models of long term random errors of gyroscopes and accelerometers in an inertial navigation system," in *Proc. IEEE Conf. Decis. Control Including 16th Symp. Adapt. Processes Special Symp. Fuzzy Set Theory Appl.*, Dec. 1977, pp. 1186–1191.

[4] Y. Wu, J. Wang, and D. Hu, "A new technique for INS/GNSS attitude and parameter estimation using online optimization," *IEEE Trans. Signal Process.*, vol. 62, no. 10, pp. 2642–2655, May 2014.

[5] X. H. Cheng and M. Zheng, "Optimization on Kalman filter parameters of SINS during initial alignment," *J. Chin. Inertial Technol.*, vol. 14, no. 4, pp. 15–16, 2006.

[6] X. Yuan and Y. Ni, "Alignment and calibration of strapdown inertial navigation system in a swaying vehicle," *Acta Aeronautica Et Astronautica Sinica*, vol. 9, pp. B338–B345, Aug. 1988.

[7] F. Sun, F. Liu, and X. Fang, "A new method of zero calibration of the strapdown inertial navigation system," in *Proc. Int. Conf. Mechatronics Automat.*, Aug. 2012, pp. 1586–1590.

[8] X. Liu, Y. Yan, Y. J. Huang, and Q. Song, "Self-alignment algorithm without latitude for SINS based on gravitational apparent motion and wavelet denoising," *J. Chin. Inertial Technol.*, vol. 24, no. 3, pp. 306–313, Jun. 2016.

[9] X. Liu, X. Xu, Y. Zhao, L. Wang, and Y. Liu, "An initial alignment method for strapdown gyrocompass based on gravitational apparent motion in inertial frame," *Measurement*, vol. 55, no. 55, pp. 593–604, 2014.

[10] X. Liu, X. Liu, Q. Song, Y. Yang, Y. Liu, and L. Wang, "A novel self-alignment method for SINS based on three vectors of gravitational apparent motion in inertial frame," *Measurement*, vol. 62, pp. 47–62, Feb. 2015.
[11] W. Chai, X. Shen, and S. Zhang, "Error analysis of analytic rough alignment for marine SDINS," *J. Harbin Eng. Univ.*, vol. 20, no. 4, pp. 46–50, Apr. 1999.
[12] C. S. Zhao, Y. Y. Qin, and L. Bai, "Analysis and test of swaying-based analytic coarse alignmen," *J. Chin. Inertial Technol.*, vol. 17, no. 4, pp. 436–440, 2009.
[13] G. M. Yan, J. Weng, L. Bai, and Y. Y. Qin, "Initial in-movement alignment and position determination based on inertial reference frame," *Syst. Eng. Electron.*, vol. 33, no. 3, pp. 618–621, 2011.
[14] Q. Li, Y. Ben, and F. Sun, "A novel algorithm for marine strapdown gyrocompass based on digital filter," *Measurement*, vol. 46, no. 1, pp. 563–571, 2013.
[15] G.-M. Yan, L. Bai, J. Weng, and Y.-Y. Qin, "SINS anti-rocking disturbance initial alignment based on frequency domain isolation operator," *J. Astronaut.*, vol. 32, no. 7, pp. 1486–1490, 2011.
[16] F. Tan, J. Xu, A. Li, and H. Zhou, "A wavelet based Kalman filter for accelerometers de-noising," *J. Wuhan Univ. Technol.*, vol. 33, no. 1, pp. 49–52, Feb. 2009.
[17] D. Georges, "The use of observability and controllability gramians or functions for optimal sensor and actuator location in finite-dimensional systems," in *Proc. 34th IEEE Conf. Decis. Control*, vol. 4, Dec. 1995, pp. 3319–3324.
[18] X.-X. Liu and X.-U. Xiao-Su, "System calibration techniques for inertial measurement units," *J. Chin. Inertial Technol.*, vol. 17, no. 5, pp. 568–571, 2009.

**XIXIANG LIU** received the B.S. degree from Nanjing Forestry University, China, in 1999, and the M.S. and Ph.D. degrees from Southeast University, China, in 2004 and 2007, respectively. He was a Lecturer and an Associate Professor with Southeast University, China, from 2007 to 2010 and 2010 to 2015, respectively, where he has been a Professor, since 2015. His research interests include inertial sensors and navigation.

**SONGBING WANG** received the B.S. degree from Anhui University, China, in 2016. He is currently pursuing the degree with Southeast University, China. His research interests include inertial sensors and navigation.

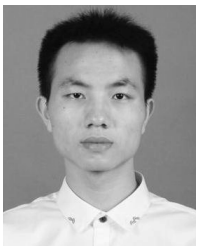

**XIAOLE GUO** received the B.S. degree from Anhui University, China, in 2017. He is currently pursuing the degree with Southeast University, China. His research interests include inertial navigation and integrated navigation.

**WENQIANG YANG** received the B.S. degree from Southeast University, China, in 2017, where he is currently pursuing the degree. His research interests include inertial navigation and inertial measurement.

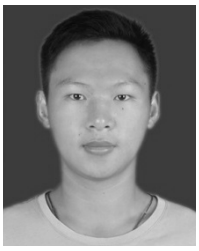

**GUANGFU XU** received the B.S. degree from Southeast University, China, in 2017, where he is currently pursuing the degree. His research interests include inertial navigation and data fusion.